ELSEVIER

Earth and Planetary Science Letters 150 (1997) 453–462

EPSL

Solar modulation of cosmogenic nuclide production over the last millennium: comparison between ^{14}C and ^{10}Be records

Edouard Bard [a,*,1], Grant M. Raisbeck [b,2], Françoise Yiou [b], Jean Jouzel [c,3]

[a] *CEREGE, Université d'Aix-Marseille III, CNRS FR-6094 / UMR-6536, Europôle de l'Arbois, BP 80, 13545 Aix-en-Provence cedex 4, France*

[b] *Centre de Spectrométrie Nucléaire et de Spectrométrie de Masse, IN2P3-CNRS, 91405 Orsay, France*

[c] *Laboratoire de Modélisation du Climat et de l'Environnement, LMCE / DSM / CEA, Orme des Merisiers, 91191 Gif-sur-Yvette cedex, France*

Received 2 December 1996; revised 28 April 1997; accepted 5 May 1997

Abstract

For about the last 30 years it has been recognized that the high frequency component of the tree rings $^{14}C/^{12}C$ record is dominated by the modulation of the cosmic ray flux by the solar wind. In particular, it has been demonstrated that the three most recent periods of low sunspot occurrence were characterized by high values of atmospheric $^{14}C/^{12}C$. During the last millennium other periods of high $^{14}C/^{12}C$ values were observed but their solar origin is still debatable. In the present work we compare these fluctuations with an independent record of cosmogenic ^{10}Be measured in ice from the South Pole to check the solar origin of the observed $^{14}C/^{12}C$ variations. In order to compare quantitatively the results obtained on ^{10}Be and ^{14}C, it is necessary to take into account the different behaviour of these two cosmogenic isotopes, and especially the damping effect of the carbon cycle in the case of ^{14}C. As an input to a 12-box numerical model we used the relative fluctuations of the ^{10}Be concentrations record measured in South Pole ice and converted it into a synthetic ^{14}C record. We took into account the fact that ^{10}Be modulation is enhanced in polar regions due to the orientation of the geomagnetic field. As expected, the fluctuations of the modelled ^{14}C record are much smaller (a factor of 20) than those observed for the raw ^{10}Be record. In addition, the variations are smoother and shifted in time by a few decades. The ^{10}Be-based ^{14}C variations closely resemble the ^{14}C measurements obtained on tree rings ($R = 0.81$). In particular, it is easy to identify periods of maximal $^{14}C/^{12}C$ which correspond to solar activity minima centred at about 1060, 1320 (Wolf), 1500 (Spörer), 1690 (Maunder) and 1820 (Dalton) yr A.D. Cross-correlation calculations suggest that there is no significant lag between the ^{10}Be-based ^{14}C and the tree-ring ^{14}C records. Our study strongly suggests the dominance of the solar modulation on the cosmonuclide production variations during the last millennium. © 1997 Elsevier Science B.V.

Keywords: solar activity; climate; cosmogenic elements; Be-10; C-14/C-12; modern

* Corresponding author. Tel.: +33 442971561. Fax: +33 442971549. E-mail: ebard@arbois.cerege.fr

1 Also at Institut Universitaire de France (IUF).

2 Tel.: +33 169415264. Fax: +33 169415268. E-mail: raisbeck@csnsm.in2p3.fr, yiou@csnsm.in2p3.fr.

3 Tel.: +33 169087713. Fax: +33 169087716. E-mail: jouzel@obelix.saclay.cea.fr.

PII S0012-821X(97)00082-4

1. Introduction

An accurate knowledge of the Sun's variability on centennial time scales is of crucial importance for the fields of astronomy and climatology. Long time series of solar variability are important targets which can be tested and ultimately reproduced by models of solar dynamics [1,2]. The variability of the short-wave solar output has a strong influence on the stratospheric photochemistry and, in particular, on compounds involved in the ozone cycle [3–6]. A knowledge of the Sun's UV fluctuations is thus needed to separate natural from anthropogenic ozone variations.

Although it has been a controversial issue for many years [7–9] a direct influence of the Sun's variability on Earth's climate has been revived recently with the definite proof of a positive relationship between the 11 year cycle of solar magnetic activity and the total radiative output measured by satellites [10,11]. A solar influence has even been invoked to explain modern variations in several climatic parameters, such as sea level atmospheric pressure [12], sea surface temperatures [13], equatorial wind patterns [14], land air temperatures [15] and strength of cyclogenesis [16]. In searching for physical mechanisms, climate modellers cautioned that simple statistical correlations could be spurious [17,18] but confirmed that solar forcing should be added to other dominant forcings, such as greenhouse gases and atmospheric aerosols [19,20].

Dramatic changes in the Sun's activity have been deduced on longer time-scales by counting sunspots with telescopes or observing aurora with the naked eye ([21,22] and references therein). Most of the attention has been focused on the prominent Maunder minimum (1645–1715 A.D.) during which almost no aurora or sunspot was observed [23,24]. This 70 yr period is roughly concomitant with the coldest temperatures of the Little Ice Age, which, again, suggests a direct solar influence on climatic variability [25–30].

Statistical studies of Sun-like stars has revealed that their distribution is bimodal: two-thirds being characterized by cyclic and/or high magnetic activity while the remainder are magnetically quiescent [31]. Further work on the relationship between brightness and magnetic activity showed a wide range of correlations between these two parameters [32]. Altogether, these studies of solar-type stars suggest the possibility that the Sun has spent about one-third of its recent history in periods of magnetic activity even lower than during the minima of the recent 11 yr sunspot cycles (although sunspots may be equally absent in both cases). Furthermore, these astronomical studies also suggest that the Sun's irradiance variations could have been much larger in the past than inferred from the 15 years of precise satellite measurements.

Unfortunately, there are no direct and reliable measurements of solar variability beyond the 17th century. Nevertheless, it has been demonstrated that the high frequency component of the tree ring $^{14}C/^{12}C$ record is dominated by solar modulation of cosmic rays [33]. Magnetic fields of the solar wind deflect the primary flux of charged cosmic particles, which leads to a reduction in ^{14}C production in the Earth's atmosphere. In particular, it was recognized that the Maunder minimum was a period of very high ^{14}C production rate (20–30% above the modern value), as deduced from a maximum of atmospheric $^{14}C/^{12}C$ at about this period [34]. During the last millennium other periods of high $^{14}C/^{12}C$ values have been observed but their solar origin awaits confirmation, since other causes can affect the atmospheric $^{14}C/^{12}C$: changes in the reservoir sizes or exchange rates of the global carbon cycle can perturb the $^{14}C/^{12}C$ of the atmosphere, which is the smallest and hence most sensitive reservoir [33,35–39].

A way of checking the solar origin of observed $^{14}C/^{12}C$ variations is to compare these fluctuations with independent records based on another cosmogenic radionuclide such as ^{10}Be measured in polar ice [40–42]. However, ^{14}C and ^{10}Be time series cannot be compared directly since the fates of these two cosmonuclides are very different after production in the atmosphere. ^{10}Be becomes fixed to aerosols and is washed out by precipitation in a matter of a year [43]. As a consequence, ^{10}Be fall-out is a marker of the regional, latitude-dependant, cosmogenic production but local, high-frequency, meteorological changes can alter its reading. By contrast, ^{14}C is oxidized and homogenized in the atmospheric $^{12}CO_2$ pool, which is connected to larger reservoirs of the carbon cycle such as biological organic matter and bicarbonate dissolved in the oceans [44]. Atmospheric $^{14}C/^{12}C$ thus follows the average global production but short-term variations are seriously damped by the carbon cycle, which requires the use of a model to quantify this inherent bias [35,39,45].

Using this approach, Beer et al. [41] compared the tree-ring ^{14}C record with a compiled profile based on ^{10}Be data measured in two Greenland ice cores: Camp Century (North Greenland) and Milcent (Central Greenland). They observed that, over the last 5000 yr, the ^{10}Be and ^{14}C signals are correlated ($R = 0.58$), which suggests that a common mechanism modulates the production of these cosmonuclides. In order to assess these conclusions we used a similar approach for a core retrieved at the South Pole, a location characterized by markedly different meteorological and precipitation regimes than the Greenland sites studied by Beer et al. [41]. In addition, our study is focused on the last millennium, for which the time scale uncertainties should be minimal (2–10 yr). Moreover, the South Pole record has two further advantages when compared to those used by Beer et al. [41]: (1) the ^{10}Be data over the last millennium were obtained in the very same core, limiting the problems of compiling records; (2) the South Pole is remote from sources of dust, which may complicate the interpretations of Greenland records [47].

2. Use of the South Pole ^{10}Be record

Core PS1 was retrieved at South Pole in 1984 and is 127 m long. Following methods pioneered by Hammer [48], the PS1 core was dated by recognizing 20 layers of impurities attributed to known volcanic eruptions and by correlation with nearby core PS14, for which seasonal variations are observed for major ions and water isotopes [49]. A nearly continuous series of ^{10}Be concentrations were measured on 1 kg ice samples every 0.8 m on average. Details can be found elsewhere concerning procedures for the chemical separation of Be [40], accelerator mass spectrometry with the Tandetron [40] and analytical results for core PS1 [46]. The precision of the dating is estimated to be between 2 and 10 yr [49] while the precision of an individual ^{10}Be concentration measurement is on the order of 7% [46]. As shown in Fig. 1, the raw ^{10}Be time series spans the last 1050

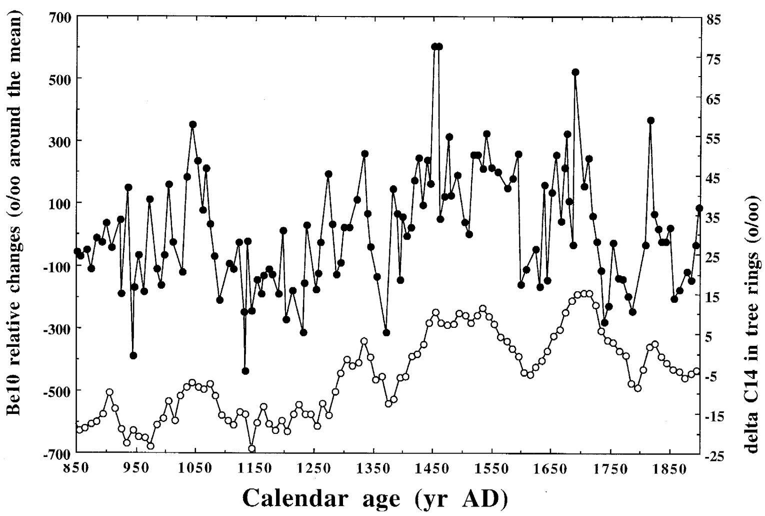

Fig. 1. Raw records of the ^{10}Be and ^{14}C variability during the last millenium. Dots and left y axis represent the relative fluctuations of the ^{10}Be concentration measured in core PS1 from South Pole [46]. Circles and right y axis represent the tropospheric $\Delta^{14}C$ values measured in American and European tree rings [50]. We excluded the 20th century from our analysis because the atmospheric $\Delta^{14}C$ can no longer be used to study the natural variations in cosmogenic production since its atmospheric concentration has been significantly altered by the anthropic combustion of fossil fuels (i.e. the so-called Suess effect, which diluted the atmospheric ^{14}C reservoir by about −30‰ in 1950 [59]).

years, exhibiting very large amplitude changes around the mean value (ca. ±300‰). Fig. 1 also shows the fractionation corrected $^{14}C/^{12}C$ values (i.e. $\Delta^{14}C$) measured on tree rings for every decade [50] (note that Fig. 1 has two different y axes). A visual correlation between the two time series does exist, as first pointed out by Raisbeck et al. [46]. However, the relative amplitudes (±300‰ vs. ±15‰), phasing, high frequencies and long term trends are clearly different, which should be quantitatively explained before attributing these fluctuations to the solar magnetic variability.

In order to take into account the damping effect of the carbon cycle we used a 12-box numerical model (Fig. 2), which is a hybrid of PANDORA [51] and the carbon cycle model used by Siegenthaler et al. [35]. The damping and phasing effects of this model depend on the frequency of production variations, as shown in Fig. 3. Century scale periodicities are damped by a factor of about 10–20 and shifted by a few decades. By contrast, decadal cycles are attenuated by a factor of 50–100 and delayed by several years.

The profile of relative ^{10}Be changes is used as a model input for the relative variations of the cosmogenic production. However, this record cannot be used directly as a proxy for the average global production because ^{10}Be measured in Antarctica ice is mainly produced at high latitudes [40]. The solar modulation should be higher at the poles than at the equator due to the orientation of the geomagnetic field. The relative amplitude of the ^{10}Be variations around the mean therefore probably overestimates the relative change in the global cosmogenic nuclide production and hence in ^{14}C. This factor was not taken into account by Beer et al. [41], who assumed

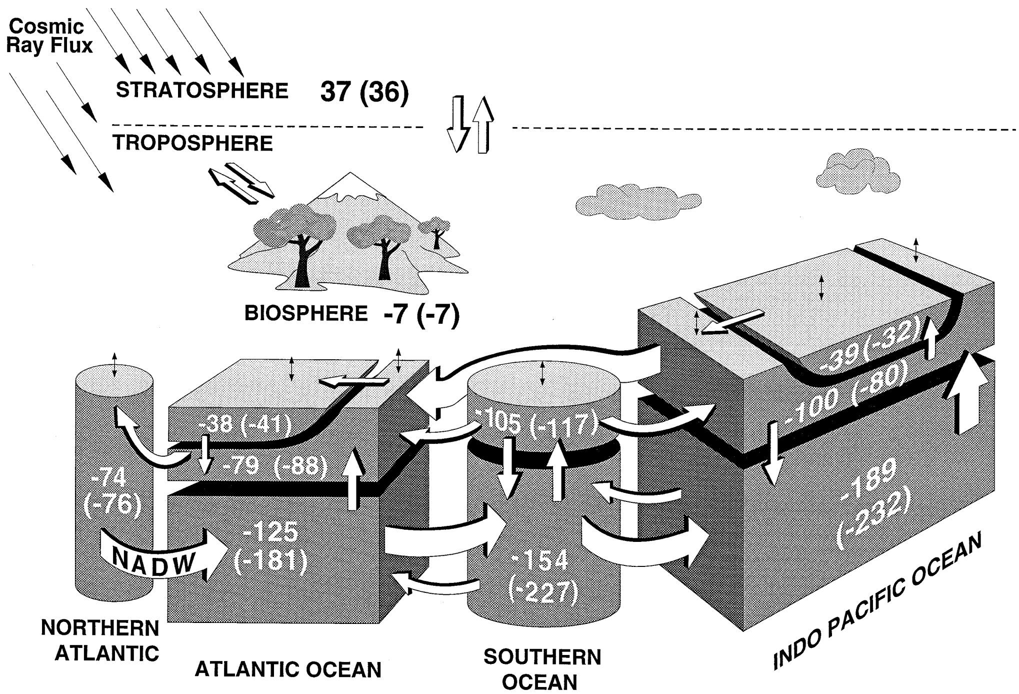

Fig. 2. The 12-box model used to simulate the carbon cycle. This numerical model is an hybrid of PANDORA [51] and the carbon cycle model used by Siegenthaler et al. [35]. The ^{14}C production occurs in the stratosphere (for two thirds) and in the troposphere (for one third). The number on each individual box is the steady-state $\Delta^{14}C$ of this particular reservoir expressed in per mil. The number in parenthesis is the steady-state $\Delta^{14}C$ for a reduced thermohaline convection (i.e. the large oceanic arrow is 20 Sv in the standard case and 10 Sv in the reduced mode). In each case the tropospheric $\Delta^{14}C$ is set to zero by definition but the reduced circulation steady state is shifted by 35‰ above the standard case.

that the ^{10}Be variability in Greenland samples is directly representative of the cosmonuclide production rate.

For the analysis of PS1 we take into account the polar enhancement by multiplying by a coefficient (PEC = Polar Enhancement Coefficient) the relative ^{10}Be variations around the mean, which are used as an input curve for the carbon cycle model. Calculations by Lal [52] indicate that, for a solar modulation at the geomagnetic pole of $\pm 17\%$ around the mean value, the equatorial modulation is less than $\pm 3\%$. By integrating over the different latitude bands, the global average modulation is about $\pm 11\%$ around the mean production, which is significantly lower than the modulation value calculated for high latitudes ($\pm 17\%$ on average for the 60–90°N zone). A theoretical PEC value can be thus estimated (i.e. $0.65 \approx 11/17$) which should be applied to the relative ^{10}Be changes in order to obtain an input curve for the global modulation of the ^{14}C production. As described below an independent estimate will be derived from statistical examination of the modelled curves obtained with a variable coefficient.

Fig. 4 shows several profiles of tropospheric Δ^{14}C simulated using the 12-box model and the relative changes in ^{10}Be as an input curve for the variable production rate. As expected, the fluctuations of the modeled ^{14}C record are much smaller (a factor of 20) than for the raw ^{10}Be profile (see Fig. 1). In addition, the variations are smoother and shifted in time by a few decades. For comparison with this synthetic Δ^{14}C we show in Fig. 4 the detrended Δ^{14}C values measured in American and European tree rings [50]. The long trend of Δ^{14}C visible in Fig. 1 is probably due to the memory of the long term geomagnetic variations and has therefore been removed before analysis of the last millennium [33,37,53].

The ^{10}Be-based ^{14}C variations closely resemble the ^{14}C measurements obtained on tree rings (R = 0.81). In particular, it is easy to identify periods of maximum Δ^{14}C which correspond to solar activity minima centred at about 1060, 1320 (Wolf), 1500 (Spörer), 1690 (Maunder) and 1820 yr A.D. (Dalton). This agreement strongly supports these periods as being times of enhanced cosmogenic nuclide production. Our agreement between simulated and observed Δ^{14}C variations appears much better (R = 0.81) than previously obtained for Greenland (R = 0.58, see [41]). Moreover, it is important to note that the correlation reported by Beer et al. in [41] is mainly due to the agreement between 3000 yr B.C. and 1000 yr A.D. For the period between 950 and 1800 yr A.D. the ^{10}Be-based Δ^{14}C record of Greenland [41]

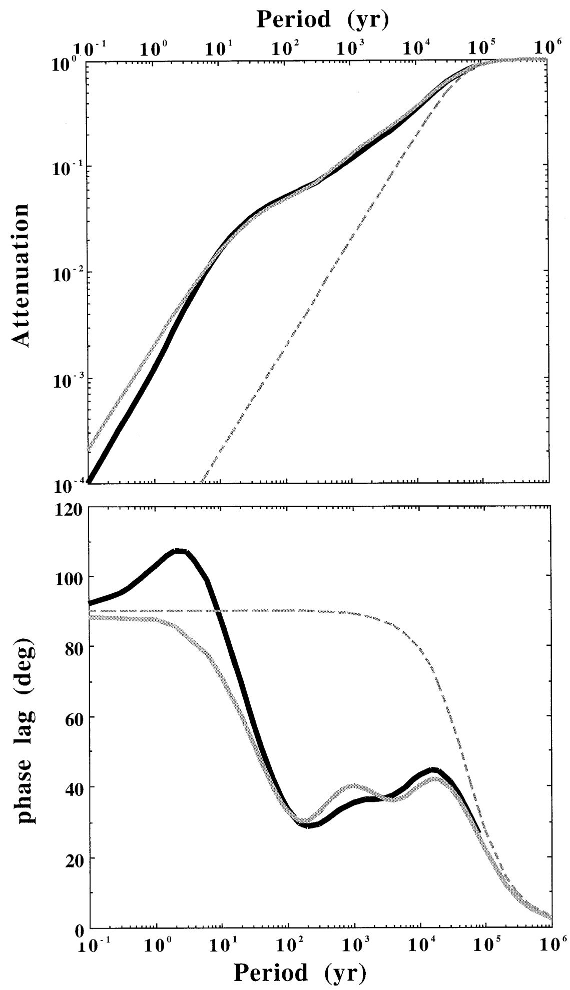

Fig. 3. Harmonic response of the tropospheric reservoir to sinusoidal changes of cosmogenic production. The upper panel shows the attenuation of Δ^{14}C change normalized to the size of the production change as a function of the period of sinusoidal production variation. The lower panel shows the phase lag of Δ^{14}C change versus the period of sinusoidal production variation. The black solid line represent the results obtained with the 12-box model shown in Fig. 2. Also shown are the harmonic responses of simple 3-box and 1-box model. The 1-box model is totally unsatisfactory to study ^{14}C variations on time scales lower than 10,000 yr whereas the 3-box model could be used down to centennial time scales.

is characterized by five excursions while the tree ring $\Delta^{14}C$ exhibits only four excursions. There is also an anomalous prominent maximum centred at about 1150 yr A.D. in the ^{10}Be-based $\Delta^{14}C$ record of Beer et al. (cf. fig. 4a in [41]). By contrast, the South Pole ^{10}Be-based $\Delta^{14}C$ record is at minimum between 1100 and 1250 yr A.D., in very good agreement with the tree-ring record (Fig. 4).

Another puzzling feature of the Greenland record [41] is the relative size of the ^{10}Be-based $\Delta^{14}C$ excursions: the amplitude of the Maunder $\Delta^{14}C$ excursion is on the order of 30‰ while the Spörer and Wolf excursions are slightly less than 10‰. As clearly shown in Fig. 4, the relative amplitude of the 1060, 1320 (Wolf), 1500 (Spörer), 1690 (Maunder) and 1820 yr A.D. (Dalton) $\Delta^{14}C$ excursions are similar in the tree ring record and the $\Delta^{14}C$ profile based on the South Pole ^{10}Be data.

The differences between the Greenland and South Pole ^{10}Be records could be due to several causes, such as the influence of 'individual' precipitation events, long term accumulation changes over a large region of the ice sheets and the contribution of ^{10}Be transported with the dust fraction. Although the correlation for the South Pole is more convincing than that observed for Greenland ice cores [41], it would still be extremely useful to compare the PS1 record with another record from the same region in Antarctica. This would help to separate the true cosmogenic production fluctuations from ^{10}Be changes linked to glaciological 'noise'.

Cross-correlation calculations show that, on average, the raw ^{10}Be fluctuations lead the $\Delta^{14}C$ records by 10–20 yr (Fig. 5a). No significant lag is detected between the ^{10}Be-based ^{14}C and the tree-ring ^{14}C records, which supports the model and assumptions about ^{10}Be variations (Fig. 5a). In addition, the correlation has been improved when compared to the cross-correlation with the raw ^{10}Be record (0.81 vs. 0.69, cf. Fig. 5a). This is probably due to the reduction of the high frequency component of the raw ^{10}Be record, which could be due to genuine changes in the cosmogenic production or to meteorological fluctuations. In both cases this ^{10}Be 'noise' is smoothed out by the carbon cycle, making the ^{10}Be-based ^{14}C profile even more similar to the observed tree-ring ^{14}C record.

Finkel and Nishiizumi [54] have recently compared the $\Delta^{14}C$ tree ring curve with a ^{10}Be profile in the GISP2 ice core from about 5000 to 8000 yr B.P.

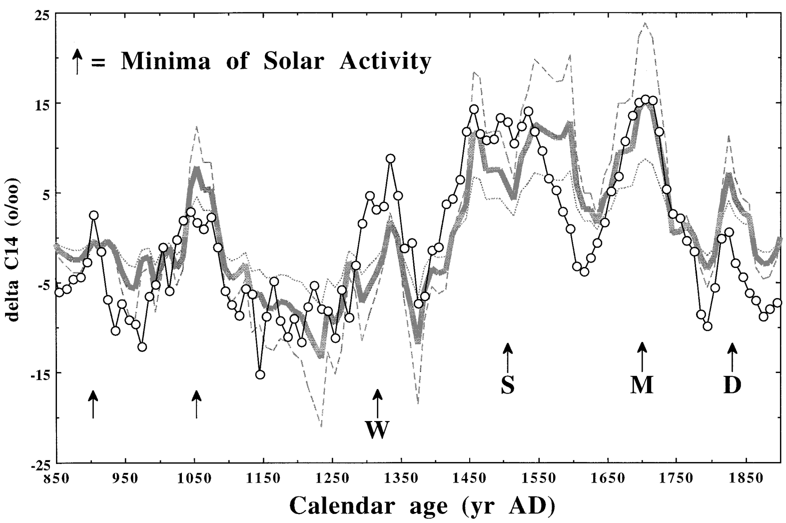

Fig. 4. Circles represent the detrended $\Delta^{14}C$ values measured in American and European tree rings [50]. Lines show the tropospheric $\Delta^{14}C$ variations simulated by using the 12-box model and the relative changes in ^{10}Be as an input curve for the variable production rate. The thick solid line shows the $\Delta^{14}C$ profile calculated with a polar enhancement coefficient of 0.7, which should be the best value according to theoretical and statistical considerations (see text). Also shown as dotted and dashed lines are profiles calculated with coefficients equal to 0.4 and 1.1, respectively.

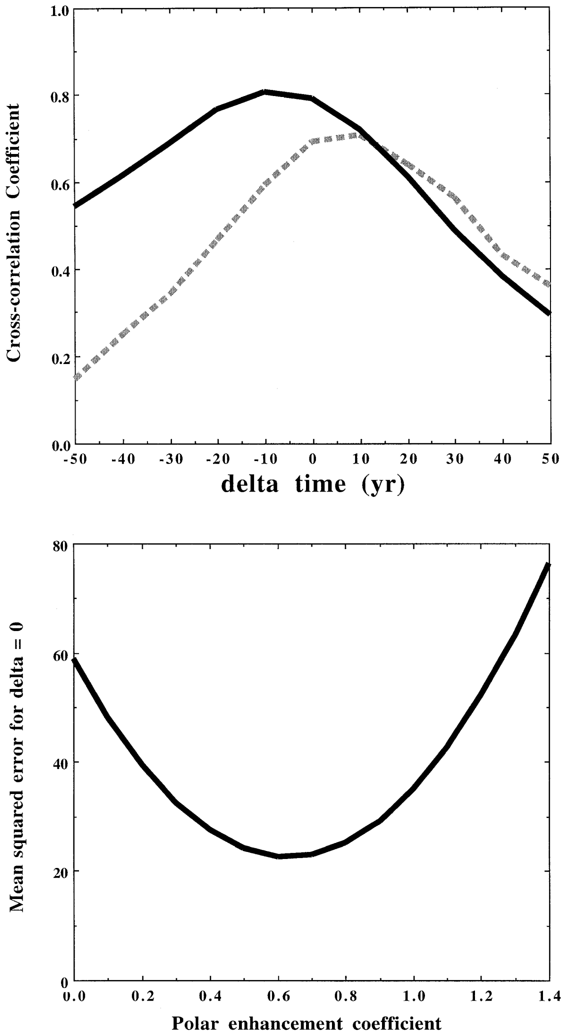

Fig. 5. Cross-correlation calculations between ^{10}Be and ^{14}C records. The upper panel shows the cross-correlation coefficient as a function of positive or negative lags. The dashed line stands for the cross-correlation between the relative ^{10}Be record and the detrended tree-ring ^{14}C profile. As expected from Fig. 3, the raw ^{10}Be changes lead the ^{14}C variations by 10–20 yr. The thick line shows the cross-correlation between the ^{10}Be-based modelled ^{14}C curve and the tree-ring ^{14}C changes. As expected, the optimal correlation is improved and there is no significant lag between the two time series. The lower panel represents the mean squared error for lag equal to zero as a function of the polar enhancement coefficient (PEC). Optimal PEC values can be found between 0.5 and 0.8, which roughly agrees with the PEC value derived from theoretical considerations (i.e. about 0.65).

They find that they must offset the two curves by 100 years to obtain the best correlation of centennial oscillations of $\Delta^{14}C$ and ^{10}Be. They suggest two possible explanations for this: (1) an error in the GISP2 time scale used; or (2) a lag between the production rate changes and the corresponding changes in $\Delta^{14}C$ in the atmosphere. As we have seen above and in Fig. 3, the latter suggestion does not seem to be tenable, unless the carbon cycle has changed dramatically between the period considered here and the early Holocene.

Model ^{10}Be-based ^{14}C curves were obtained for various values of the polar enhancement coefficient. In order to estimate an optimum we plotted the mean squared error for lag equal to zero, since all cross-correlograms are equivalent to the one presented in Fig. 5a. The optimum PEC value is 0.6 which is slightly lower than the one derived by theoretical considerations (i.e. about 0.65). However, both calculations and assumptions suffer from inherent uncertainties and we consider this agreement as satisfactory. For example, we have assumed that the ocean was at steady state during the last millennium, which is a first order approximation. The 12-box model shown in Fig. 2 allows variation in North Atlantic Deep Water (NADW) production. As an example, the atmospheric $\Delta^{14}C$ calculated with the modern (20 Sv) and halved (10 Sv) NADW productions are different by 35‰ at steady state. A 35‰ increase in the atmospheric $\Delta^{14}C$ would thus be expected if this large NADW reduction lasted at least 1500 yr. This is probably what happened during the dramatic Younger Dryas cold event (see fig. 4 in [38]). However, if a similar reduction in NADW flux lasted for only a century, the atmospheric $\Delta^{14}C$ wiggle would be much smaller (i.e. about 6‰). Although it is not possible to rule out slight changes in the deep ocean ventilation during the last millennium, it is unlikely that they have been more than about 10–15%. Consequently, this cause cannot account for more than 1–2‰ of the total variability (30‰ in Fig. 4), which could also explain an error of about 0.1 in the PEC optimization. Fully coupled ocean–atmosphere general circulation models including the carbon cycle (e.g. [55]) should be used in future to identify and evaluate feedbacks within the climate system and carbon cycle forced by the solar variability.

3. Conclusions

The South Pole record complements the study by Beer et al. [41], who quantified a significant correlation ($R = 0.58$) between ^{14}C in tree rings and ^{10}Be measured in Greenland ice cores. Our study, focused on the last millennium at the South Pole, documents an even better correlation ($R = 0.81$) between the fluctuations of these two cosmonuclides. These observations in both polar regions strongly suggest the dominance of the solar modulation on the cosmonuclide production during the last millennium. In particular, there is no need to invoke other causes to explain the centennial variability in the atmospheric $\Delta^{14}C$.

Furthermore our study agrees with the conclusion by Steig et al. [56] that most ^{10}Be atoms trapped in Antarctica ice were produced at high latitudes and that it is important to take this effect into account when comparing quantitatively the ^{14}C and ^{10}Be fluctuations observed at different latitudes. This is in conflict with previous assumption by Mazaud et al. [57] that ^{10}Be is essentially well mixed in the atmosphere.

The period between 950 and 1900 yr A.D. is characterized by five cosmonuclide production maxima which probably correspond to minima of solar activity. These century scale events are centred at 1060, 1320, 1500, 1690, 1820 yr A.D. The common variations in the ^{10}Be and ^{14}C productions documented in this study could ultimately be used as a proxy for solar radiative output, provided that astronomers and solar dynamicists are able to improve the understanding of the relationship between star brightness and magnetic activity.

Correlation of a ^{10}Be-simulated ^{14}C curve with that observed in tree rings could also be used to date ice cores in regions (such as the Antarctic plateau) where other dating methods are not feasible [58]. We are presently using such a procedure to date the Vostok ice core for most of the Holocene.

Acknowledgements

We thank J. Guiot for his help in calculating the cross-correlation matrix, J.R. Petit for helpful discussions, C.U. Hammer and M. Stuiver and two anonymous referees for reviews of the manuscript. This study was supported by programme ‘‘Dynamique et bilans de la Terre’’ of INSU. Tandetron operation is supported by the CNRS, CEA and IN2P3. ***[FA]***

References

[1] K.H. Schatten, A model for solar constant secular changes, Geophys. Res. Lett. 15 (1988) 121–124.
[2] P. Foukal, J. Lean, An empirical model of total solar irradiance variation between 1874 and 1988, Science 247 (1990) 556–558.
[3] J.C. Gille, C.M. Smythe, D.F. Heath, Observed ozone response to varations in solar ultraviolet radiation, Science 225 (1984) 315–317.
[4] G.M. Keating, J. Nicholson III, G. Brasseur, A. De Rudder, U. Schmailzl, M. Pitts, Detection of stratospheric HNO_3 and NO_2 response to short-term solar ultraviolet variability, Nature 322 (1986) 43–46.
[5] S. Chandra, The solar UV related changes in total ozone from a solar rotation to a solar cycle, Geophys. Res. Lett. 18 (1991) 837–840.
[6] J.D. Haigh, The role of stratospheric ozone in modulating the solar radiative forcing of climate, Nature 370 (1994) 544–546.
[7] A.J. Meadows, A 100 years of controversy over sunspots and weathers, Nature 256 (1975) 95–97.
[8] R.H. Dicke, Is there a chronometer hidden deep in the Sun?, Nature 276 (1978) 676–680.
[9] M. Stuiver, Solar variability and climatic change during the current millennium, Nature 286 (1980) 868–871.
[10] R.C. Willson, H.S. Hudson, Solar luminosity variations in solar cycle 21, Nature 332 (1988) 810–812.
[11] J.R. Hickey, B.M. Alton, H.L. Kyle, D. Hoyt, Total solar irradiance measurements by ERB/Nimbus-7: A review of nine years, Space Sci. Rev. 48 (1988) 321–342.
[12] P.M. Kelly, Solar influence on North Atlantic mean sea level pressure, Nature 269 (1977) 320–322.
[13] G. Reid, Influence of solar variability on global sea surface temperatures, Nature 329 (1987) 142–143.
[14] K. Labitzke, H. van Loon, Associations between the 11-year solar cycle, the QBO and the atmosphere, I, The troposphere and stratosphere in the northern hemisphere winter, J. Atmos. Terrestr. Phys. 50 (1988) 197–206.
[15] E. Friis-Christensen, K. Lassen, Length of the solar cycle: an indicator of solar activity closely associated with climate, Science 254 (1991) 698–700.
[16] B.A. Tinsley, Solar wind mechanism suggested for weather and climate change, EOS Trans. Am. Geophys. Union 75 (32) (1994) 369–374.
[17] I.N. James, P.M. James, Ultra-low-frequency variability in a simple atmospheric circulation model, Nature 342 (1989) 53–55.
[18] P.M. Kelly, T.M.L. Wigley, The influence of solar forcing trends on global mean temperature since 1861, Nature 347 (1990) 460–462.

[19] J.E. Hansen, A.A. Lacis, Sun and dust versus greenhouse gases: an assessment of their relative roles in global climate change, Nature 346 (1990) 713–719.
[20] P.M. Kelly, T.M.L. Wigley, Solar cycle length, greenhouse forcing and global climate, Nature 360 (1992) 328–330.
[21] J.A. Eddy, The Maunder minimum. The reign of Louis XIV appears to have been a time of real anomaly in the behavior of the sun, Science 192 (1976) 1189–1202.
[22] S.M. Silverman, Secular variation of the aurora for the past 500 years, Rev. Geophys. 30 (4) (1992) 333–351.
[23] J.J.D. deMairan, Traité physique et historique de l'Aurore Boréale, Imprimerie Royale, Paris, 1733.
[24] R.W. Maunder, A prolonged sunspot minimum, Knowledge 17 (106) (1894) 173–176.
[25] J. Lean, A. Skumanich, O. White, Estimating the Sun's radiative output during the maunder minimum, Geophys. Res. Lett. 19 (1992) 1591–1594.
[26] E. Nesme-Ribes, A. Mangeney, On a plausible physical mechanism linking the maunder minimum to the little ice age, Radiocarbon 34 (2) (1992) 263–270.
[27] E. Nesme-Ribes, E.N. Ferreira, R. Sadourny, H. Le Treut, Z.X. Li, Solar dynamics and its impact on solar irradiance and the terrestrial climate, J. Geophys. Res. 98 (1993) 18923–18935.
[28] J. Lean, D. Rind, Solar variability: implications for global change, EOS 75 (1) (1994) 1–6.
[29] J. Lean, J. Beer, R. Bradley, Reconstruction of solar irradiance since 1610: Implications for climate change, Geophys. Res. Lett. 22 (1995) 3195–3198.
[30] T.J. Crowley, K.-Y. Kim, Comparison of proxy records of climate change and solar forcing, Geophys. Res. Lett. 23 (1996) 359–362.
[31] S. Baliunas, R. Jastrow, Evidence for long-term brightness changes of solar-type stars, Nature 348 (1990) 520–522.
[32] G.W. Lockwood, B.A. Skiff, S.L. Baliunas, R.R. Radick, Long-term solar brigthness changes estimated from a survey of Sun-like stars, Nature 360 (1992) 653–655.
[33] M. Stuiver, P.D. Quay, Changes in atmospheric carbon-14 attributed to a variable sun, Science 207 (1980) 11–19.
[34] M. Stuiver, Variations in radiocarbon concentration and sunspot activity, J. Geophys. Res. 66 (1961) 273–276.
[35] U. Siegenthaler, M. Heimann, H. Oeschger, ^{14}C variations caused by changes in the global carbon cycle, Radiocarbon 22 (2) (1980) 177–191.
[36] T.-H. Peng, Changes in ocean ventilation rates over the last 7000 years based on ^{14}C variations in the atmosphere and oceans, Radiocarbon 31 (3) (1989) 481–492.
[37] M. Stuiver, T.F. Braziunas, Sun, ocean, climate and atmospheric $^{14}CO_2$: an evaluation of causal and spectral relationships, Holocene 3 (4) (1993) 289–305.
[38] T. Goslar, M. Arnold, E. Bard, T. Kuc, M.F. Pazdur, M. Ralska-Jasiewiczowa, K. Rozanski, N. Tisnerat, A. Walanus, B. Wicik, K. Wieckowski, High concentration of atmospheric ^{14}C during the Younger Dryas cold episode, Nature 377 (1995) 414–417.
[39] T.F. Stocker, D.G. Wright, Rapid changes in ocean circulation and atmospheric radiocarbon, Paleoceanography 11 (1996) 773–795.
[40] G.M. Raisbeck, F. Yiou, M. Fruneau, J.M. Loiseaux, M. Lieuvin, J.C. Ravel, C. Lorius, Cosmogenic ^{10}Be concentrations in Antarctic ice during the past 30,000 years, Nature 292 (1981) 825–826.
[41] J. Beer, U. Siegenthaler, G. Bonani, R.C. Finkel, H. Oeschger, M. Suter, W. Wölfli, Information on past solar activity and geomagnetism from ^{10}Be in the Camp Century ice core, Nature 331 (1988) 675–679.
[42] J. Beer, A. Blinov, G. Bonani, R.C. Finkel, H.J. Hofmann, B. Lelmann, H. Oeschger, A. Sigg, J. Schwander, T. Staffelbach, B. Stauffer, M. Suter, W. Wölfli, Use of ^{10}Be in polar ice to trace the 11-year cycle of solar activity, Nature 347 (1990) 164–166.
[43] G.M. Raisbeck, F. Yiou, M. Fruneau, J.M. Loiseaux, M. Lieuvin, J.C. Ravel, Cosmogenic $^{10}Be/^{7}Be$ as a probe of atmospheric transport processes, Geophys. Res. Lett. 8 (1981) 1015–1018.
[44] W.F. Libby, Radiocarbon Dating. The University of Chicago Press, 1955.
[45] H.L. deVries, Variation in concentration of radiocarbon with time and location on Earth, Proc. Koninkl. Ned. Akad. Wetenschap. (1958) 94–102.
[46] G.M. Raisbeck, F. Yiou, J. Jouzel, J.R. Petit, ^{10}Be and ^{2}H in polar ice cores as a probe of the solar variability's influence on climate, Philos. Trans. R. Soc. London Ser. A 300 (1990) 463–470.
[47] S. Baumgartner, J. Beer, G. Wagner, P. Kubik, M. Suter, G.M. Raisbeck, F. Yiou, ^{10}Be and dust, Nucl. Instrum. Methods B123 (1997) 296–301.
[48] C.U. Hammer, Past volcanism revealed by Greenland ice sheet impurities, Nature 270 (1977) 482–486.
[49] R.J. Delmas, S. Kirchner, J.M. Palais, J.-R. Petit, 1000 years of explosive volcanism recorded at South Pole, Tellus 44B (1992) 335–350.
[50] M. Stuiver, B. Becker, High-precision decadal calibration of the radiocarbon time scale, AD 1950–6000 BC, Radiocarbon 35 (1993) 35–65.
[51] W.S. Broecker, T.-H. Peng, Carbon cycle: 1985 Glacial to interglacial changes in the operation of the global carbon cycle, Radiocarbon 28 (2A) (1986) 309–327.
[52] D. Lal, Theoretically expected variations in the terrestrial cosmic-ray production rates of isotopes, in: Solar–Terrestrial Relationships and the Earth Environment in the Last Millennia, vol. XCV, Soc. Italiana di Fisica, Bologna, 1988, pp. 216–233.
[53] E. Bard, B. Hamelin, R.G. Fairbanks, A. Zindler, Calibration of the ^{14}C timescale over the past 30,000 years using mass spectrometric U–Th ages from Barbados corals, Nature 345 (1990) 405–410.
[54] R.C. Finkel, N. Nishiizumi, ^{10}Be and ^{36}Cl concentrations in the GISP2 ice core compared with $\Delta^{14}C$ in tree rings, EOS Trans. Am. Geophys. Union 77 (46) (1996) F428.

[55] E. Maier-Reimer, U. Mikolajewicz, A. Winguth, Future ocean uptake of CO_2: interaction between ocean circulation and biology, Clim. Dynam. 12 (1996) 711–721.

[56] E.J. Steig, P.J. Polissar, M. Stuiver, P.M. Grootes, R.C. Finkel, Large amplitude solar modulation cycles of ^{10}Be in Antartica: implications for atmospheric mixing processes and interpretation of the ice core record, Geophys. Res. Lett. 23 (1996) 523–526.

[57] A. Mazaud, C. Laj, M. Bender, A geomagnetic chronology for Antarctic ice accumulation, Geophys. Res. Lett. 21 (1994) 337–340.

[58] G.M. Raisbeck, F. Yiou, Dating by cosmogenic isotopes ^{10}Be, ^{26}Al and ^{41}Ca, in: E. Roth, B. Poty (Eds.), Nuclear Methods of Dating, CEA, Paris, 1989, pp. 353–378.

[59] H. Suess, Radiocarbon concentration in modern wood, Science 122 (1955) 415–417.